OPEN

Citation: Cell Death and Disease (2014) 5, e1116; doi:10.1038/cddis.2014.82

www.nature.com/cddis

A stress-induced cellular aging model with postnatal neural stem cells

C-M Dong[1,2,3,8], X-L Wang[1,8], G-M Wang[1,8], W-J Zhang[4], L Zhu[1], S Gao[1], D-J Yang[1], Y Qin[1], Q-J Liang[2,5], Y-L Chen[6], H-T Deng[6], K Ning[1,7], A-B Liang[*,4], Z-L Gao[*,2,5] and J Xu[*,1]

Aging refers to the physical and functional decline of the tissues over time that often leads to age-related degenerative diseases. Accumulating evidence implicates that the senescence of neural stem cells (NSCs) is of paramount importance to the aging of central neural system (CNS). However, exploration of the underlying molecular mechanisms has been hindered by the lack of proper aging models to allow the mechanistic examination within a reasonable time window. In the present study, we have utilized a hydroxyurea (HU) treatment protocol and effectively induced postnatal subventricle NSCs to undergo cellular senescence as determined by augmented senescence-associated-β-galactosidase (SA-β-gal) staining, decreased proliferation and differentiation capacity, increased G0/G1 cell cycle arrest, elevated reactive oxygen species (ROS) level and diminished apoptosis. These phenotypic changes were accompanied by a significant increase in p16, p21 and p53 expression, as well as a decreased expression of key proteins in various DNA repair pathways such as xrcc2, xrcc3 and ku70. Further proteomic analysis suggests that multiple pathways are involved in the HU-induced NSC senescence, including genes related to DNA damage and repair, mitochondrial dysfunction and the increase of ROS level. Intriguingly, compensatory mechanisms may have also been initiated to interfere with apoptotic signaling pathways and to minimize the cell death by downregulating Bcl2-associated X protein (BAX) expression. Taken together, we have successfully established a cellular model that will be of broad utilities to the molecular exploration of NSC senescence and aging.

Cell Death and Disease (2014) **5,** e1116; doi:10.1038/cddis.2014.82; published online 13 March 2014
Subject Category: Neuroscience

Aging is characterized by progressive declines in the physiology and functionality of adult tissues and can manifest nine common hallmarks: genomic instability, telomere attrition, epigenetic alterations, loss of proteostasis, deregulated nutrient sensing, mitochondrial dysfunction, cellular senescence, stem cell exhaustion and altered intercellular communication.[1] At cellular levels, these age-dependent declines can arise from the accumulation of damage and erosion to cellular macromolecules including proteins, RNA and DNA, usually a result of cellular stress and environmental insults.[2] Of these, DNA damage accrual and insufficient DNA repair often accompanied by oxidative stress and mitochondrial dysfunction is a principal factor contributing to cell senescence and aging.[3] Conversely, DNA repair pathways delay cell senescence and aging by maintaining genomic integrity.[4] Perhaps the fundamental importance of DNA damage control in aging is best illustrated by the fact that human monogenic progeroid syndromes are caused almost exclusively by mutations in DNA repair genes whose deficiency also result in premature aging in mouse models.[5] DNA damage accumulation may also be a major force to drive resident stem cell aging and eventual exhaustion. Genetic lesions with DNA repair pathway components in mouse models profoundly impact resident stem cell integrity through various mechanisms.[5] For example, DNA damage accumulates in aged hematopoietic stem cells (HSCs) and defects in DNA damage repair pathway cause HSC deficiency and hematopoietic abnormalities.[6,7] Besides, DNA lesions in stem cells could propagate both to daughter stem cells and to downstream lineages. Therefore, the capability of stem cells to cope with

[1]East Hospital, Tongji University School of Medicine, Shanghai 200120, People's Republic of China; [2]Tenth People's Hospital Affiliated to Tongji University, Shanghai, People's Republic of China; [3]Department of Anatomy and Neurobiology, Jiangsu Key Laboratory of Neuroregeneration, Nantong University, Nantong, People's Republic of China; [4]Department of Hematology, Tongji Hospital of Tongji University School of Medicine, Shanghai, People's Republic of China; [5]Advanced Institute of Translational Medicine, Tongji University School of Medicine, Shanghai, People's Republic of China; [6]School of Life Sciences, Tsinghua University, Beijing, People's Republic of China and [7]Department of Neuroscience, Sheffield Institute for Translational Neuroscience (SITraN), University of Sheffield, Sheffield, UK
*Corresponding author: A Liang, Department of Hematology, Tongji Hospital of Tongji University School of Medicine, 389 Xincun Road, Shanghai 200065, People's Republic of China. Tel: +86 21 66111019; Fax: +86 21 66111019; E-mail: lab7182@tongji.edu.cn
or Z Gao, Advanced Institute of Translational Medicine, Tongji University School of Medicine, 1239 Siping Road, Shanghai 200092, People's Republic of China. Tel: +86 21 55897392; Fax: +86 21 55897392; E-mail: zhengliang_gao@tongji.edu.cn
or J Xu, East Hospital, Tongji University School of Medicine, 150 Jimo Road, Shanghai 200120, People's Republic of China. Tel: +86 21 65982412; Fax: +86 21 65985616; E-mail: xunymc2000@yahoo.com
[8]These authors contributed equally to this work.
Keywords: aging; neural stem cells; cellular senescence model; stress; DNA damage
Abbreviations: NSC, neural stem cell; CNS, central neural system; HU, hydroxyurea; ROS, reactive oxygen species; HSC, hematopoietic stem cell; PRDX1, peroxiredoxin 1; SOD2, superoxide dismutase 2; COX2, cytochrome *c* oxidase subunit II; SVZ, subventricular zone; HBSS, Hank's balanced saline solution; IPA, Ingenuity Pathway Analysis; HR, homologous recombination; NHEJ, nonhomologous end joining; SA-β-gal, senescence-associated-β-galactosidase; DSB, DNA double-strand break
Received 08.10.13; revised 05.1.14; accepted 07.1.14; Edited by A Stephanou

DNA damage will have profound impact on the genomic integrity of stem cells and their progenies.

Adult neural stem cells (NSCs) are essential for brain homeostasis but suffer from proliferative declines and cellular senescence with age.[8] The decreased proliferation,[9,10] increased G0/G1 cell cycle arrest and reduced neuronal neurogenesis[11] gradually result in the loss of repair and regeneration capacity, contributing to neural aging and disorders such as olfactory dysfunction,[12] spatial memory deficits[13] and neurodegenerative diseases.[14,15] Various intrinsic factors can modulate this functional decline and thus brain aging.[16–19] For example, the age-dependent increase of the senescence regulators (e.g., p16) contributes to the diminishing of aged NSC pool.[20] Adult neurogenesis is also sensitive to environmental stress (e.g., DNA damage). A single dose of 10 Gy radiation exposure led to long-lasting cognitive impairment[21] and deficiency in DNA double-strand break (DSB) repair could result in precocious neurogenesis and ultimately decreased neuronal production.[22] Despite these progresses, molecular characterizations of the responses of adult NSCs to DNA damage and their functional importance are largely absent.[23] Equally lacking is whether and how adult NSCs have developed compensatory mechanisms to combat the devastating consequences caused by excessive DNA damage and aging.

The aging of NSCs is a difficult subject to study, on one hand, because of the sparsity and no easy accessibility of *in vivo* experimental materials and, on the other hand, because of the lack of proper models to manipulate the key genes and examine the molecular mechanisms within relatively short periods of time. Thus, establishing *in vitro* models of NSC aging becomes vital to elucidate NSC aging mechanisms. Hydroxyurea (HU) initially used as an anti-neoplastic drug[24] represses the ribonucleotide reductase and decreases the production of deoxyribonucleotides. Thus, it can incur DSBs near replication forks and function as a DNA replication inhibitor for both nuclear and mitochondrial DNA, causing cellular and mitochondrial stress and dysfunction.[25] It can induce senescence-like changes in various cell lines but in NSCs its effect remains undetermined.[26]

In the current study, utilizing HU treatment we have optimized and carefully characterized a cellular NSC aging model that could recapture many of the aging attributes. Further proteomics analysis unraveled molecular networks related to diverse aging hallmarks, suggesting the broad utilities of our cellular model for mechanistic dissection of NSC and neural aging.

Results

Establishment and characterization of primary NSC culture. NSCs from the subventricular zone (SVZ) of postnatal day 7 (P7) mice were cultured in the presence of epidermal growth factor (EGF) and basic fibroblast growth factor (bFGF) and formed neurospheres *in vitro* (Supplementary Figure S1A). During subculturing, the NSC culture maintained their stem cell characteristics and stained positively for Nestin and SOX2 (Supplementary Figure S1B). It can also undergo differentiation toward neurons, astrocytes and oligodendrocytes (Supplementary Figures S2 and S3).

Persistent DNA damage induced by HU treatment. To determine the optimal dosing of HU to induce DSBs and cell senescence, NSCs were treated for 1 and 12 h at three different doses of 0.5, 8 and 20 mM. The treatment with 20 mM HU caused cell death as manifested by DNA fragmentation and apoptotic bodies (Figure 1a), but low and medium dosing of HU did not obviously change the NSC culture. We then examined the extent of DSBs by quantifying γH2AX foci that form at the sites of DNA damage. Untreated NSCs displayed a basal level of γH2AX foci. The treatment of 0.5 mM HU for 1 or 12 h or of 8 mM HU for 1 h induced an immediate increase in γH2AX foci number that declined rapidly and returned to the baseline at 36 h post treatment. The treatment of 8 mM HU for 12 h triggered rapid increase in γH2AX foci number but that failed to go down even at 36 h post treatment (Figures 1b and c).

Establishment of a NSC aging model using mild DNA damage treatment. Our results demonstrated that the low dosing of HU only induced transient DSBs, whereas the high dosing of HU was incompatible with NSC survival. Therefore, for further experimentations, we opted to use mild dosing of HU (8 mM HU, 12 h) that produced persistent DSBs (Figure 1c).

To verify whether we can establish a cellular NSC aging model with 8 mM HU treatment, a series of characterizations were performed. First, we carried out neurosphere formation assays and our results showed that the ratio of neurosphere formation was markedly reduced in the HU-treated group (Figures 2a and b), suggesting the self-renewal capacity of NSCs is significantly impaired by the treatment. Upon exposure to 1% FBS, the majority of the cells in both groups spontaneously differentiated into GFAP$^+$ cells with typical astrocyte morphology (Figures 2c and d). A small fraction of the cells became Tuj1$^+$ neurons with multipolarized processes. The proportion of neurons in HU-treated cells was significantly decreased (Figures 2c and d), indicating that the neuronal differentiation ability of NSCs was significantly compromised by the treatment.

To test whether this mild DNA damage treatment causes cell senescence in NSCs, we stained the NSCs with the senescence-associated-β-galactosidase (SA-β-gal), an established senescence marker. HU treatment induced robust β-galactosidase expression (Figure 3a). The percentage of SA-β-gal positive NSCs increased from 8.39% in the control group to 26.63% in the HU-treated one (Figure 3b). Cell senescence is usually accompanied by increased intracellular reactive oxygen species (ROS) level. Consistent with that, the HU-treated NSCs had higher ROS level than the control cells (Figures 3c and d).

DNA damage usually induces cell cycle arrest and apoptosis. To assay that, we performed fluorescence-activated cell sorting (FACS) experiment. As determined by propidium iodide (PI) staining (Figure 3e), HU treatment induced a significant increase in G0/G1 phases and a significant decrease in G2/M populations (Figures 3f and g). Intriguingly, mild HU treatment reduced the level of apoptosis in NSCs compared with the control treatment (Figure 3h).

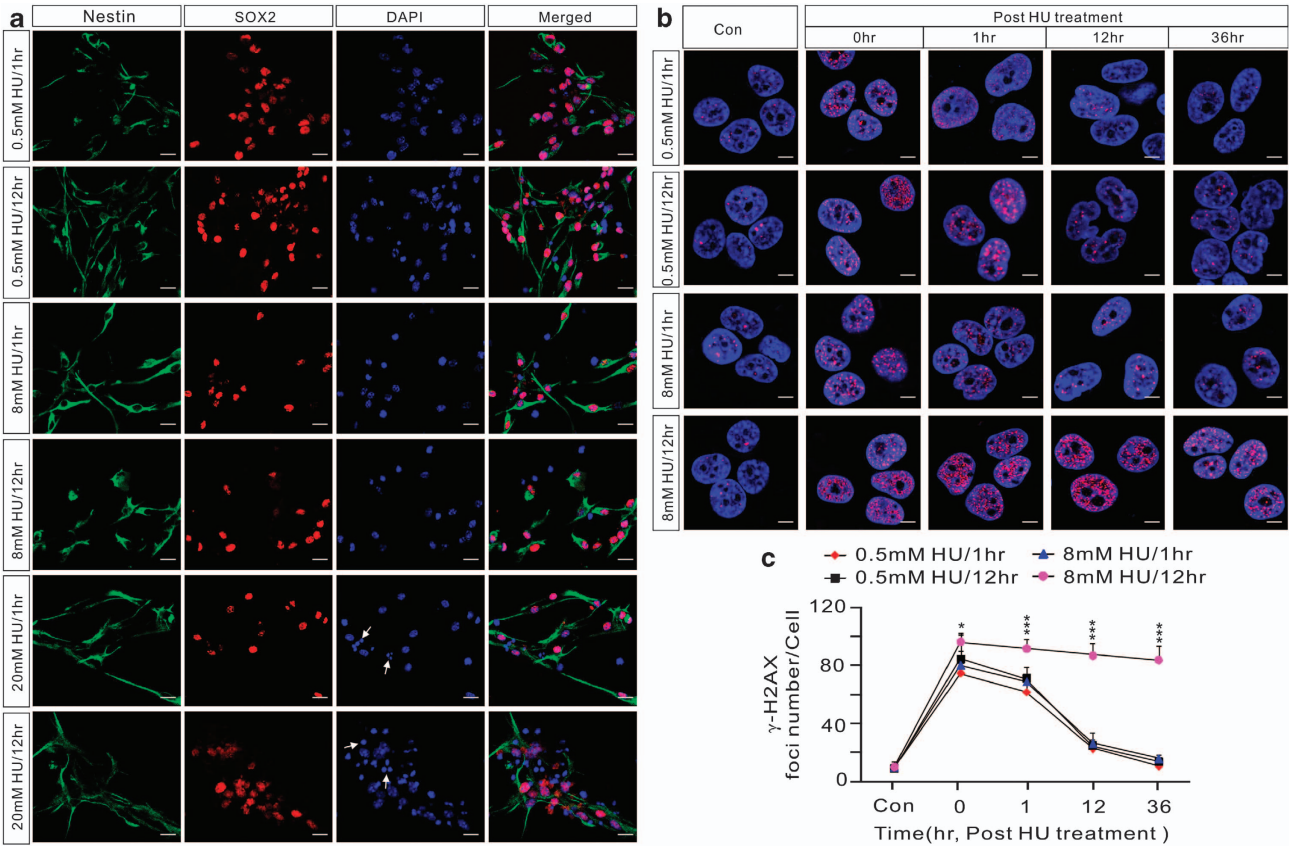

Figure 1 Persistent DNA damage induced by HU treatment. (**a**) NSCs were treated with 0.5, 8 and 20 mM HU for 1 or 12 h respectively and stained with Nestin, SOX2 and DAPI post treatment. The white arrows point to apoptotic bodies. Scale bar: 20 μm. (**b**) Formation of DNA double-strand breaks in NSCs post HU treatment. NSCs were treated with 0.5 and 8 mM HU for 1 or 12 h and allowed to recover until 36 h post treatment. Cells were fixed and stained for γH2AX foci (red) at the indicated time points post HU treatment. Scale bar: 5 μm. (**c**) Graphical depiction of the number of γH2AX foci in NSCs treated with 0.5 or 8 mM HU over 36 h. Data are expressed as mean ± S.E. from three independent experiments. $^*P<0.05$, $^{***}P<0.001$, two-way ANOVA with Fisher's *post hoc* test (see Supplementary Table S1)

Aging-related genes and pathways altered in the model. Mild HU treatment not only diminished NSC proliferative capability and neuronal differentiation potential but also induced senescence-related phenotypes, implying successful establishment of a cellular aging model. However, it remained to be determined whether our model can recapitulate molecular mechanisms related to aging. Thus, we next sought to validate the model through analyzing known aging-related genes and pathways.

p53/p21 pathway is crucial in cellular response to DNA damage[27] and p16 is a cyclin-dependent kinase inhibitor. Both are major pathways controlling cell cycle arrest and cell senescence.[28] Consistent with our expectation, mild HU treatment led to a significant increase in the expression of p16, p21 and p53 as unraveled by QRT-PCR (Figure 3i) and western blot (Figure 3j) analyses.

One major effect of mild HU treatment is the persistent DSBs that might result from compromised DNA damage repair. Therefore, we examined the expression of some major genes for DNA damage repair including key components of the homologous recombination (HR) repair pathway (e.g., xrcc2 and xrcc3) and the nonhomologous end joining (NHEJ) repair pathway (e.g., ku70, xrcc4 and ligase4). HU treatment decreased the expression of both the HR and NHEJ pathway genes (Figures 3k–n), which could be underlying HU-induced persistent DNA damage, leading to NSC senescence.

Taken together, our HU treatment system effectively recaptured broad aspects of aging at both phenotypical and molecular levels and shall constitute a valid cellular aging model for further exploration.

Proteomic analysis unraveling major molecular pathways related to NSC aging. The establishment of the cellular aging model enables us to use genome-wide approach and systematically explore the mechanisms that count for the aging-related declines in an unbiased manner. To demonstrate such utilities, we performed quantitative proteomic analysis and sought to identify key proteins and pathways modulating the aging process. Our analysis produced 1209 distinct proteins. With a 2.0-fold cutoff, 48 proteins were found to be upregulated and 19 proteins were downregulated (Figure 4 and Supplementary Table S2). Functionally, these proteins are mainly associated with cellular aging, cell cycle arrest, mitochondrial integrity, ROS and stress response, DNA damage response and cell death (Figures 4 and 5).

We then performed bioinformatic analyses on the differentially expressed proteins using the DAVID Bioinformatics

Resource 6.7 (http://david.abcc.ncifcrf.gov/) and Ingenuity Pathway Analysis (IPA; Ingenuity Systems: http://www.ingenuity.com). The majority of the differentially expressed proteins are located in the lysosome (37%), the nucleus (26%) and the mitochondrion (10%) (Figure 5a). These proteins predominantly fall in the canonical pathways related to mitochondrial dysfunction and energy metabolism (Figure 5b). The top five enriched biological processes ($P<0.001$) are nucleic acid metabolism, small molecule biochemistry, energy production, lipid metabolism and post-translational modification (Figure 5c). For physiological system development and function, behavior, hair and skin development and nervous system development function were among the top (Figure 5d). Importantly, upon HU treatment, many of the proteins underwent expression changes in a highly correlated manner and readily formed some canonical pathways associated with certain aging hallmarks such as mitochondrial dysfunction (e.g., superoxide dismutase 2 (SOD2), cytochrome *c* oxidase subunit II (COX2), NADH dehydrogenase 1β subcomplex 9 (NDUFB9), NDUFB10, NADH dehydrogenase 1α subcomplex 2 (NDUFA2), NDUFAF4 and ATP synthase-H$^+$ transporting-mitochondrial F1 complex-α subunit 1 (ATP5A1))[29–33] as well as deregulated nutrient sensing and metabolisms (tricarboxylic acid cycle cycle (TCA), pyruvate fermentation lactate and β-fatty acid oxidation I) (Figure 5b).

To extrapolate major cellular functional networks altered in HU-treated NSCs, we performed IPA pathway analysis. Again, several networks relevant to aging hallmarks were readily grouped together. The most significant network contains 26 proteins relating to DNA replication, recombination and repair, ROS, energy production and nucleic acid metabolism (Figure 6a). Importantly, the expression patterns of these proteins are highly correlated with the cellular phenotypes observed. For example, peroxiredoxin 1 (PRDX1) and SOD2 was decreased in the HU-treated cells (Figure 6b), consistent with the increased ROS and NSC senescence. We then validated the proteomic data by RT-PCR and QRT-PCR. As shown in Figures 6c and d, the relative expression level of PRDX1 and SOD2 mRNA decreased by 30 and 70% in the HU-treated cells, in perfect accord with the quantitative proteomic results.

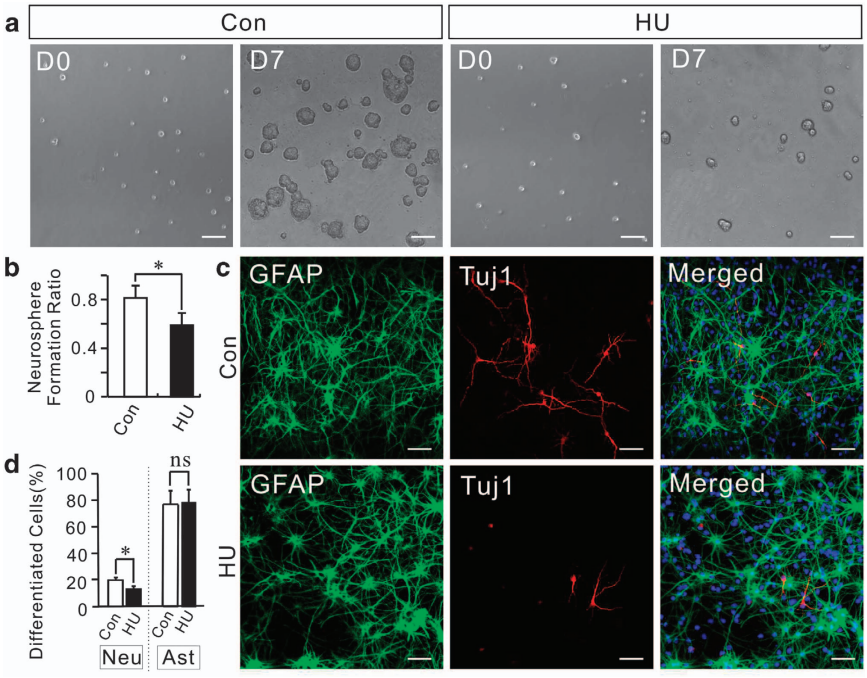

Figure 2 Proliferation and differentiation of HU-treated NSCs. (**a**) *In vitro* proliferative capacity of NSCs assayed by colony formation experiment. Representative images of neurospheres from control (Con) and HU-treated (HU) cells. The number of neurospheres formed after 1 week was counted. D0 shows the plated NSCs after single-cell dissociation at day 0. D7 shows the neurosphere formed after 7 days of culturing. Scale bar: 60 μm. (**b**) Statistics for the ratio of neurosphere formation after 7 days *in vitro*. Mean ± S.E. from three independent experiments. *$P<0.05$, Student's *t*-test. (**c**) *In vitro* differentiation of neurospheres from control and HU-treated cells as determined by the neuronal marker (Tuj1) and the astrocyte marker (GFAP). Cells showed a decreased proportion of neural progeny in the HU-treated group. Scale bar: 50 μm. (**d**) Statistics for the percentage of Tuj1$^+$ and GFAP$^+$ cells out of all cells formed from control and HU-treated cells. Ast, astrocyte; Neu, neuron. Mean ± S.E. from three independent experiments. *$P<0.05$, Student's *t*-test

Figure 3 Phenotypic and molecular characterization of 8 mM HU-treated NSCs. (**a**) Images of SA-β-gal$^+$ NSCs with or without HU treatment. (**b**) Statistics of the percentage of SA-β-gal$^+$ NSCs, mean ± S.E. *$P<0.05$, Student's *t*-test, Scale bar: 50 μm. (**c**) ROS were detected using dihydroethidium (DHE) fluorescence. (**d**) ROS level was normalized to that of control cells with statistics expressed as mean ± S.E. *$P<0.05$, Student's *t*-test. Scale bar: 60 μm. (**e–h**) In NSCs, 8 mM HU treatment resulted in irreversible cell cycle arrest and reduced apoptosis. Cell cycle analysis with (**e**) FACS analysis and (**f–h**) percentages of G0/G1, G2/M and apoptotic subpopulations are presented as mean of percentage ± S.E. (**i** and **j**) QRT-PCR analysis of p16, p21 and p53 expression normalized by GAPDH and western blotting analysis of p16 and p21 expression. (**k–n**) QRT-PCR analysis of HR (xrcc2 and brca1) and NHEJ (ku70, ligase4 and xrcc4) gene expression normalized by GAPDH (**k** and **l**), and western blotting analysis of the related proteins (**m** and **n**). Values represent mean ± S.E. of two independent samples conducted in triplicate. *$P<0.05$; **$P<0.01$, Student's *t*-test

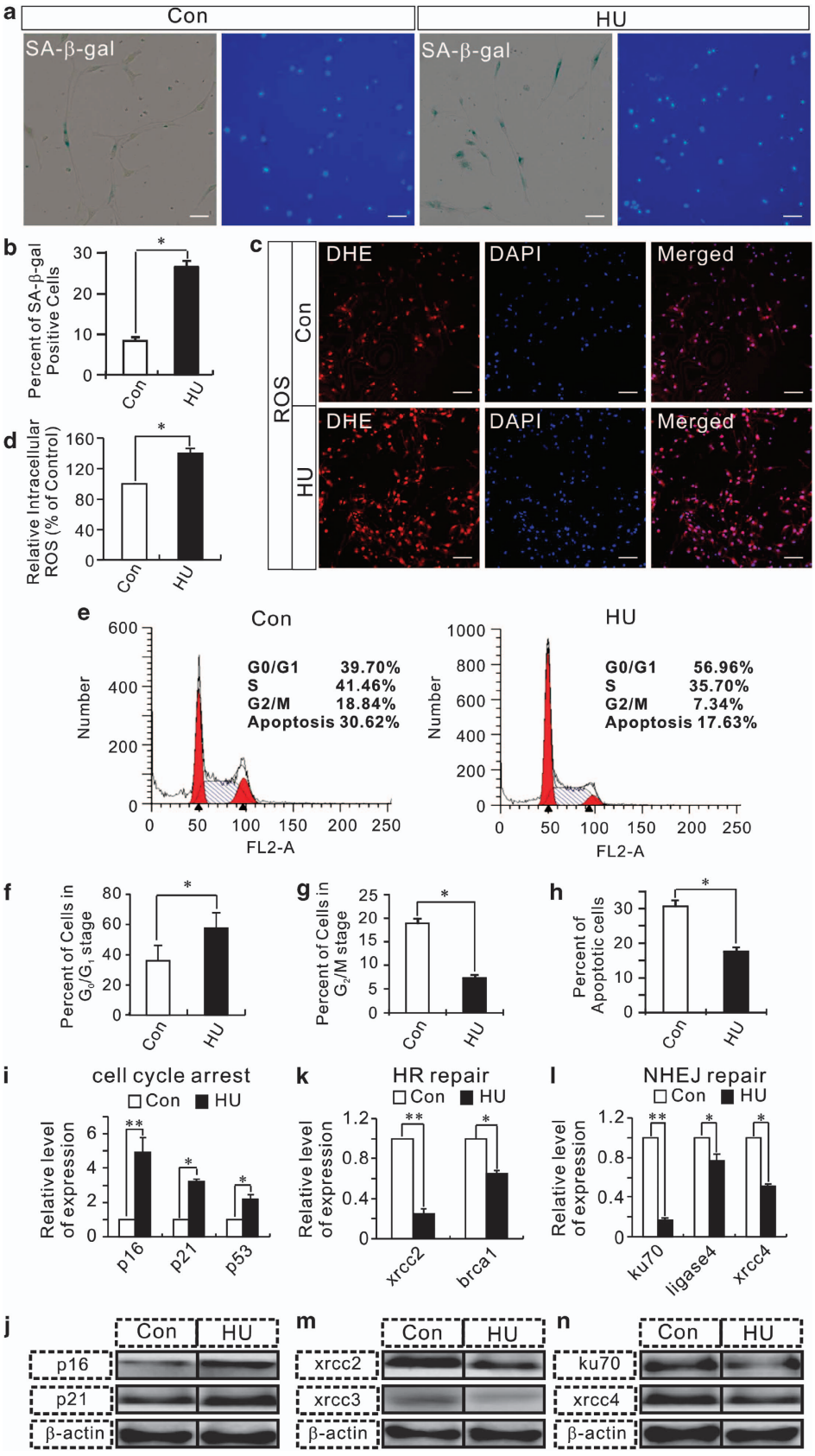
a
Con
HU
SA-β-gal
SA-β-gal
b
Percent of SA-β-gal Positive Cells
30
20
10
0
Con
HU
c
ROS
Con
HU
DHE
DAPI
Merged
DHE
DAPI
Merged
d
Relative Intracellular ROS (% of Control)
160
120
80
40
0
Con
HU
e
Con
G0/G1 39.70%
S 41.46%
G2/M 18.84%
Apoptosis 30.62%
HU
G0/G1 56.96%
S 35.70%
G2/M 7.34%
Apoptosis 17.63%
Number
FL2-A
f
Percent of Cells in G0/G1 stage
g
Percent of Cells in G2/M stage
h
Percent of Apoptotic cells
i
cell cycle arrest
Con
HU
Relative level of expression
p16
p21
p53
k
HR repair
xrcc2
brca1
l
NHEJ repair
ku70
ligase4
xrcc4
j
p16
p21
β-actin
m
xrcc2
xrcc3
β-actin
n
ku70
xrcc4
β-actin

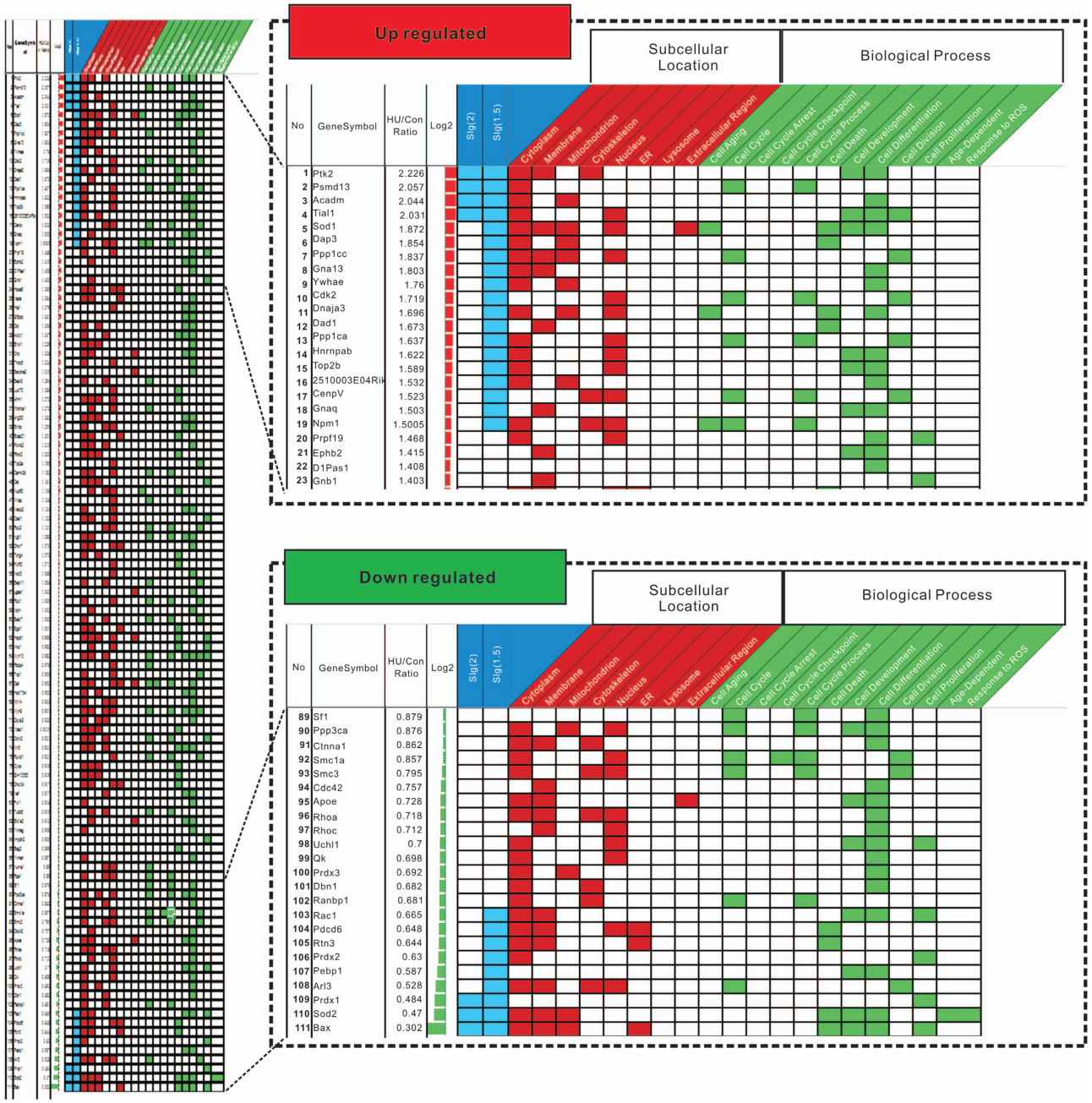

Figure 4 Heatmap analysis of differentially expressed proteins post HU treatment. The GO information was obtained from Gene Ontology Annotation database. The ratio of protein expression between HU and control groups was presented as log2 values and represented by the lengths of the bar. The red and green bars stand respectively for the upregulated and the downregulated. The subcellular location and biological function of each protein are allocated and indicated respectively by the red- and green-colored spaces

Taken together, our proteomic exploration unraveled some major aging-related pathways of both known and novel players and showcased the potential to elucidate aging-associated molecular mechanisms with the help of our cellular model based on HU treatment of NSCs (Figure 6e).

Discussion

Aging and aging-related diseases represent a major social and economic burden to the modern society. Numerous efforts have been geared toward this direction, aiming at the discovery of innovative therapeutic strategies to slow down or reverse this process. However, aging by nature is a time-dependent incremental progress and thus it is both time consuming and challenging to perform mechanistic experimentations, begging scalable aging models to enable systematic and in-depth investigations within reasonable time frames.

Among the different organs, central neural system (CNS) presents particular challenging for the aging study, both for its

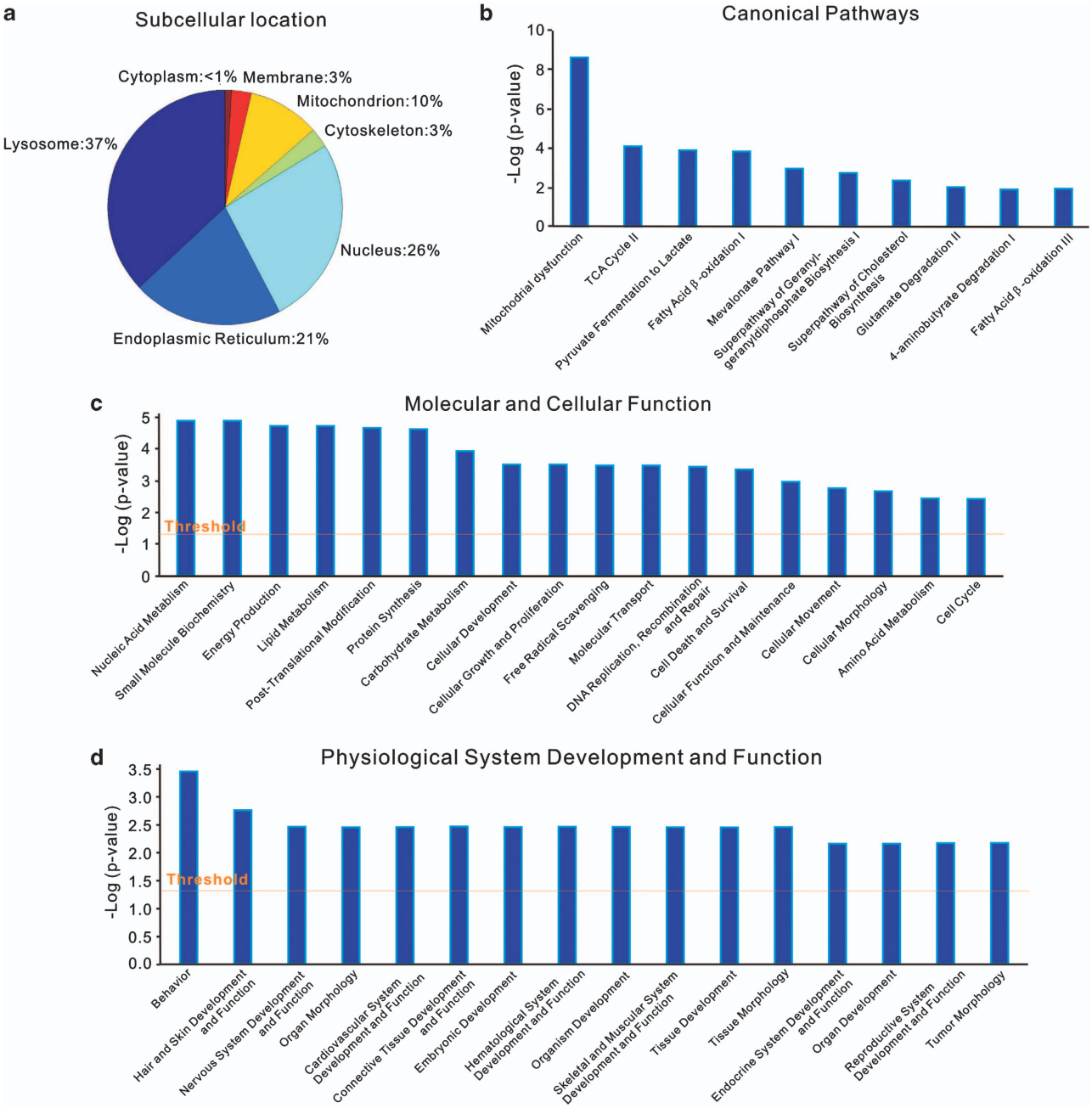

Figure 5 Biological function analysis of the differentially expressed proteins post HU treatment. (**a**) The cellular component annotations of differentially expressed proteins with GO analysis from DAVID database. (**b**) Top canonical pathways altered post HU treatment with mitochondrial dysfunction being the most significant one. (**c**) Molecular and cellular function analysis of the differentially expressed proteins with nucleic acid metabolism, small-molecule biochemistry and energy production being the most significant ones. (**d**) Physiological system development and function analysis of the differentially expressed proteins with the behavior, hair and skin development and nervous system development being the most significant ones

very complexity and its very importance. As such, despite observations indicating the involvement of some major pathways in CNS and NSC aging, studies in these areas remain scarce and essentially incoherent. Thus, it is of paramount importance to establish NSC aging models and enable systematic investigations in an unbiased manner.

In the present study, we treated postnatal NSCs with 8 mM HU for 12 h and successfully established an accelerated cellular aging model. HU treatment not only induced irreversible cell cycle arrest and senescence-like morphology, but also caused elevated expression of senescence-related genes and dysfunction of DNA damage repair machinery. Consequently, the proliferative and neurogenic differentiative capacity of NSCs was also impaired. Furthermore, chronic DNA damage accumulation and decline of DNA repair capacity were accompanied by increased intracellular ROS level and reduced apoptosis (Figure 6e). These results together demonstrate that premature senescence of cultured

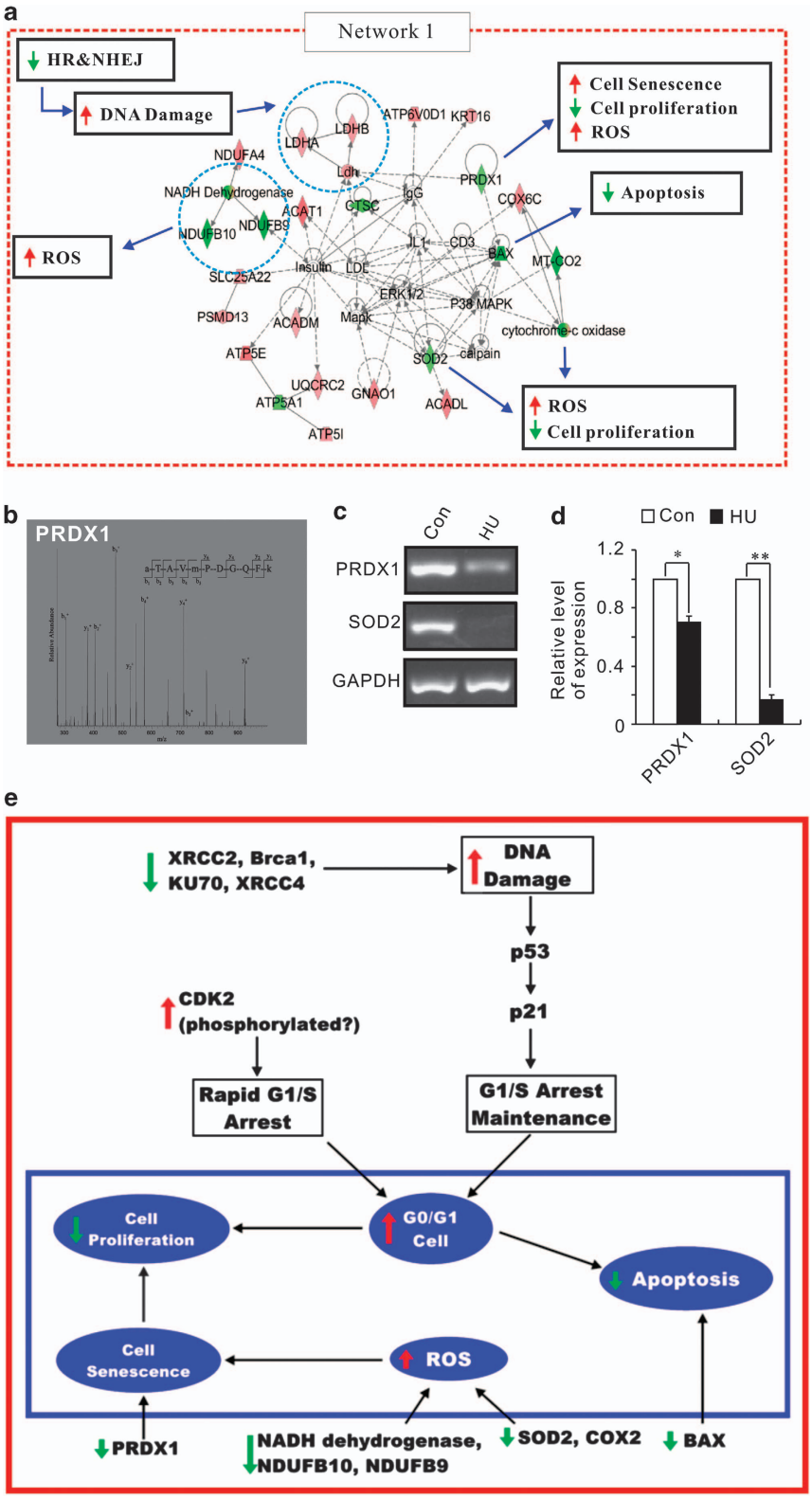

Figure 6 Candidate genes and pathways identified through the NSC cellular aging model associated with aging characteristics. (**a**) The key regulatory networks underlying the HU-induced aging model. Proteomic data were imported into the IPA and interacting pathways were constructed with red representing an increase and green indicating a decrease in protein expression. The color intensity represents the degree of expression change with the solid and dashed lines respectively indicating direct and indirect interactions. (**b**) The mass spectra image for PRDX1 with LC – MS/MS analysis. (**c** and **d**) Verification of PRDX1 and SOD2 expression by RT-PCR (**c**) and QRT-PCR (**d**) with GAPDH as an internal control. The data are presented as mean ± S.E. from three independent experiments. (**e**) The schematic diagram outlines the key players and pathways that may mechanistically contribute to the phenotypes in our NSC aging model

NSCs induced by HU treatment can recapitulate key elements of aging *in vivo* and thus can serve as a useful aging model.

Our success of establishing NSC aging model enables systematic investigations into the molecular mechanisms of aging in an unbiased manner. As described above, DNA damage and thus genomic instability is an inherent nature of our aging model utilizing HU treatment. Naturally, we have readily detected increases in DNA damage and changes in DNA damage repair pathways (both HR and NHEJ) in HU-treated NSCs (Figures 3k–n). Cell senescence was a major phenotypic evidence for our aging model accompanied by an upregulation of many key aging and senescence regulators including p16, p21 and p53 (Figures 3i and j). The expression of p16 increases in aged mouse and human tissues[34] and the increased expression of p16, p21 and p53 all led to decreased NSC proliferation and neurogenesis.[20] In response to persistent DNA damage, the expression of p53, p21 and p16 increased, ultimately contributing to halting cell proliferation to allow DNA repair to occur. We also observed a decrease in PRDX1 expression in response to the HU treatment (Figure 6c). Intriguingly, PRDX1-deficient fibroblasts manifested proliferation deficiency and were more sensitive to oxidative DNA damage.[35] Mechanistically loss of PRDX1 accelerated mouse embryonic fibroblast (MEF) senescence by increasing the phosphorylation of p53 (Ser19) upon persistent DNA damage.[36] The role of PRDX1 in the neural system is completely unknown and it is speculative that reduced PRDX1 expression is a causal factor leading to NSC senescence.

Another hallmark of our NSC aging model is the increase in intracellular ROS level (Figures 3c and d). We found a twofold decrease in the expression of SOD2 in HU-treated NSCs (Figures 6c and d). SOD2 is a main antioxidant enzyme that scavenges ROS in the inner mitochondrial matrix and acts as a first line of defense against mitochondrial oxidative stress.[37] Mitochondrial oxidative damage resulted from SOD2 deficiency promoted cellular senescence and aging phenotypes in the skin.[38] In concert, mice lacking PRDX1 manifested a shortened lifespan owing to the severe hemolytic anemia beginning at $\sim$9 months, characterized by an increase in erythrocyte ROS, protein oxidation and hemoglobin instability.[35] Furthermore, NDUFB9 and NDUFB10, components of the mitochondrial complex I, were both downregulated in HU-treated NSCs[39] (Figure 6a) and their deficiency was associated with mitochondrial dysfunction.[40] ROS level was thought to increase with age because of accumulating mitochondrial damage in a self-perpetuating cycle.[41] ROS-induced mitochondrial impairment further resulted in increased ROS production that led to even more mitochondrial damage.[2] As unraveled by our proteomic analysis, a large number of proteins misregulated in our aging model are related to mitochondrial dysfunction (Figure 5b), implying the importance of mitochondrial homeostasis for aging and the power of our cellular model.

The increased ROS can also exacerbate the DNA damage repair and response.[42] Besides the DNA damage response pathways identified through RT-PCR analyses, our unbiased proteomic analysis revealed that in HU-treated NSCs the most enriched network (network 1) of 26 proteins is related to DNA replication, recombination and repair, ROS, energy production and nucleic acid metabolism (Figure 6a). Together with recent reports,[43,44] network 1 suggest that p38 MAPK pathway may play an important role in NSC senescence. Increased DNA damage and ROS are capable of activating p38 MAPK pathway that in turn can upregulate senescence genes such as p16.[4]

As is known, ROS are involved in many cellular metabolic and signaling processes.[45] Insights from our analysis of the NSC aging model suggest the altered ROS pathways may work in concert with changes in TCA cycle, pyruvate fermentation lactate and β-fatty acid oxidation I (Figure 5b), leading to deregulated nutrient sensing and metabolism, and consequentially accelerated aging.

HU treatment induced irreversible cell cycle arrest and impairment in the NSC proliferation and neurogenic potential, in line with a stem cell senescence and exhaustion phenotype (Figures 2 and 3). However, intriguingly, NSC apoptosis decreased post HU treatment as unraveled by FACS analysis (Figure 3e). This counterintuitive observation suggests an adaptive response: NSCs adopt a compromised state to prevent from being completely eliminated upon sublethal insults such as (mild HU treatment-induced) persistent DNA damage, largely mimicking the aging process. Indeed, similar observations have been noted in other stem cell compartments such as HSCs.[46] As well, our proteomic analysis revealed that the expression of BAX, a major pro-apoptotic protein, was significantly downregulated in HU-treated NSCs (Figure 6a), lending strong support to the notion of an adaptive response.

Taken together, our data seem to support the following model during HU-induced NSC aging. DNA damage induces the expression of p53, p21 and p16, and the accompanying repression of CDK2 (Figure 6e). Together, these changes drive the NSCs to enter G1/S cell cycle arrest and help to mitigate the devastating consequences induced by DNA damage and allow time to repair. Contingent on the cellular contexts, G1-arrested cells may enter apoptosis, senescence (permanent quiescence) or reversible quiescence capable to go back to cell cycle and proliferate. In our model, upon mild dosing of HU, DNA damage caused cell cycle arrest and overwhelmed DNA damage repair pathways whose downregulation further magnified the DNA damage effects. Concordantly, DNA damage-associated stress (e.g., increased ROS level) and the repression of anti-ROS/-cell senescence genes (e.g., SOD2 and PRDX1) precipitated the arrested NSCs to senescence, during which the adaptive downregulation of BAX contributed to the decreased apoptosis.

As afore-discussed, our current study demonstrates broad utilities of the HU-induced NSC aging model to mechanistically dissect the diverse aspects of aging from genomic instability, deregulated nutrient sensing and mitochondrial dysfunction to cellular senescence and stem cell exhaustion. Although this aging model has helped to reveal some major networks underlying NSC aging, many questions remain, such as given an aging insult, how organisms/cells make their decisions to die or to compromise and adapt, how the status and context of NSCs (e.g., quiescence and the age of the cells) may influence the outcome of aging insults, how the different aging insults are being sensed and the different pathways being triggered, whether there are NSC-specific

aging pathways and what they are, and whether and how aged NSCs can be rejuvenated. Apparently, as an *in vitro* system, this model is unlikely to faithfully recapture every aspect of aging such as altered intercellular communication. As well, we are yet to test whether this model will be of any usage to mimic the telomere attrition, epigenetic alterations and loss of proteostasis – the remaining hallmarks of aging. Nor have we validated our model using complementary approaches. Finally, the relevance of our *in vitro* model with physiological aging needs to be comprehensively justified and ultimately shall be subjected to *in vivo* scrutinization.

In conclusion, we have developed a protocol and established an aging model using postnatal NSCs that can largely recapitulate the *in vivo* aging characteristics. Based on this model, we have identified genes associated with persistent DNA damage, cell senescence, G1/S arrest, increased ROS and compromised proliferation and differentiation. These findings have rendered it possible to explore NSC aging mechanisms in detail. Importantly, the availability of this aging model provides us the opportunity to systematically discover the key aging-related genes and elucidate how they work together to endow the aging phenotypes and may someday lead to innovative strategies to fight against aging and the associated disorders.

Materials and Methods

Neurosphere culture. Primary NSC culture was derived from postnatal day 7 mice. The SVZ was isolated and enzymatically dissociated in Hank's balanced saline solution buffer (HBSS) (Invitrogen, Grand Island, NY, USA) containing 1 mg/ml trypsin (Invitrogen) at 37°C for 10 min followed by 5 min of centrifugation at 350 × *g* upon trypsin inhibition (Invitrogen). The isolated cells were washed with HBSS and resuspended in DMEM/F12 medium (Invitrogen) with 2% B27 (Invitrogen), 20 ng/ml EGF (R&D Systems, Minneapolis, MN, USA), 20 ng/ml bFGF (R&D Systems) and 2 mM glutamax (Invitrogen). Neurospheres formed over 3 days of incubation with 5% CO_2 at 37°C. Subculturing was done every 3–4 days. Experiments were performed with cultured cells between passages 3 and 7 except those otherwise indicated.

HU treatment. Cells were seeded at 1×10^5 cells per ml in 24-well plates (Corning Incorporated, Corning, NY, USA), treated with HU (Sigma, St. Louis, MO, USA) at a concentration of 0.5, 8 or 20 mM, and incubated at 37°C until the collection time points.

SA-β-gal assay. Cellular senescence was determined by SA-β-gal staining.[47] Staining was performed using the Senescence Cells Histochemical Staining Kit (Sigma) according to the manufacturer's guidelines with DAPI as counterstaining. Positive staining was evaluated after 12–16 h incubation at 37°C in a CO_2-free atmosphere. The blue stained cells from 10 different fields were counted with results presented as a percentage of positive cells.

Western blot analysis. Cultured NSCs were washed with ice-cold PBS and lysed with 2 × SDS lysis buffer. Protein concentrations were determined by the BCA protein assay kit (Pierce, Rockford, IL, USA). Proteins were separated on 8% SDS-polyacrylamide gels (Bio-Rad Laboratories, Inc., Hercules, CA, USA) and transferred to a PVDF membrane (Millipore, Billerica, MA, USA). Membranes were blocked in 5% non-fat milk powder in TBS-T (0.1% Tween-20 in TBS), and incubated with primary antibodies overnight at 4°C. After washing in TBS-T, membranes were incubated with HRP-conjugated secondary antibodies (Invitrogen) for 1 h at room temperature with signals detected using ECL Super Signal (Pierce). Quantifications were done using Image-Quant Software (Molecular Dynamics, Sunnyvale, CA, USA). The primary antibodies used include rabbit anti-p16 (Abcam, Cambridge, MA, USA), anti-p21 (Abcam), anti-ku70 (Abcam), anti-Xrcc2 (Abclonal Technology, Wuhan, China), anti-Xrcc3 (Abclonal Technology), anti-Xrcc4 (Abclonal Technology) and mouse anti-βactin (Sigma).

Protein pathway analysis. GO annotation of the identified proteins was done using DAVID (V6.7: http://david.abcc.ncifcrf.gov/). Differentially expressed proteins were analyzed using IPA (Ingenuity Systems: http://www.ingenuity.com). The overrepresented biological functions, molecular networks and canonical pathways were generated based on information in the Ingenuity Pathways Knowledge Base.

Statistical analysis. Data were analyzed by Student's *t*-test and one-way analysis of variance (ANOVA) followed by *post hoc* multiple comparison tests. Significance was accepted at $P < 0.05$.

Conflict of Interest

The authors declare no conflict of interest.

Acknowledgements. This work was supported by the Ministry of Science and Technology of China (2010CB945200, 2011CB966200, 2012CB966300); the National Natural Science Foundation of China (81070910, 81200832, 81270615, 31371497); Projects of International Cooperation and Exchanges NSFC (81261130318); National program for support of Top-notch young professionals; the Fundamental Research Funds for the Central Universities; Tongji University Talents Training Program (2011KJ051); New Century Excellent Talents in University (NCET-10-0606); Jiangsu Nature College Foundation (13KJB310011); 51th China Postdoctoral surface Project (2012M510890); Shanghai Postdoctoral Research Funding Scheme of 2012 (12R21416200).

Author contributions

CD, XW and GW: conception and design, collection and assembly of data, data analysis and interpretation and manuscript writing; WZ, LZ, SG, DY, YQ, KN and QL: helped with study design, data analysis and interpretation; YC and HD: quantitative proteomic analysis; AL, ZG and JX: conception and design, data analysis and interpretation, financial support, manuscript writing and final approval of manuscript.

1. López-Otín C, Blasco MA, Partridge L, Serrano M, Kroemer G. The hallmarks of aging. *Cell* 2013; **153**: 1194–1217.
2. Lombard DB, Chua KF, Mostoslavsky R, Franco S, Gostissa M, Alt FW. DNA repair, genome stability, and aging. *Cell* 2005; **120**: 497–512.
3. Signer RA, Morrison SJ. Mechanisms that regulate stem cell aging and life span. *Cell Stem Cell* 2013; **12**: 152–165.
4. Campisi J. Aging, cellular senescence, and cancer. *Annu Rev Physiol* 2013; **75**: 685–705.
5. Moskalev AA, Shaposhnikov MV, Plyusnina EN, Zhavoronkov A, Budovsky A, Yanai H *et al.* The role of DNA damage and repair in aging through the prism of Koch-like criteria. *Ageing Res Rev* 2013; **12**: 661–684.
6. Nijnik A, Woodbine L, Marchetti C, Dawson S, Lambe T, Liu C *et al.* DNA repair is limiting for haematopoietic stem cells during ageing. *Nature* 2007; **447**: 686–690.
7. Rossi DJ, Bryder D, Seita J, Nussenzweig A, Hoeijmakers J, Weissman IL. Deficiencies in DNA damage repair limit the function of haematopoietic stem cells with age. *Nature* 2007; **447**: 725–729.
8. Kuhn HG, Dickinson-Anson H, Gage FH. Neurogenesis in the dentate gyrus of the adult rat: age-related decrease of neuronal progenitor proliferation. *J Neurosci* 1996; **16**: 2027–2033.
9. Luo J, Daniels SB, Lennington JB, Notti RQ, Conover JC. The aging neurogenic subventricular zone. *Aging Cell* 2006; **5**: 139–152.
10. Maslov AY, Barone TA, Plunkett RJ, Pruitt SC. Neural stem cell detection, characterization, and age-related changes in the subventricular zone of mice. *J Neurosci* 2004; **24**: 1726–1733.
11. Rao MS, Hattiangady B, Abdel-Rahman A, Stanley DP, Shetty AK. Newly born cells in the ageing dentate gyrus display normal migration, survival and neuronal fate choice but endure retarded early maturation. *Eur J Neurosci* 2005; **21**: 464–476.
12. Enwere E, Shingo T, Gregg C, Fujikawa H, Ohta S, Weiss S. Aging results in reduced epidermal growth factor receptor signaling, diminished olfactory neurogenesis, and deficits in fine olfactory discrimination. *J Neurosci* 2004; **24**: 8354–8365.
13. Drapeau E, Mayo W, Aurousseau C, Le Moal M, Piazza PV, Abrous DN. Spatial memory performances of aged rats in the water maze predict levels of hippocampal neurogenesis. *Proc Natl Acad Sci USA* 2003; **100**: 14385–14390.
14. Winner B, Kohl Z, Gage FH. Neurodegenerative disease and adult neurogenesis. *Eur J Neurosci* 2011; **33**: 1139–1151.
15. Ming GL, Song H. Adult neurogenesis in the mammalian brain: significant answers and significant questions. *Neuron* 2011; **70**: 687–702.

16. Lugert S, Basak O, Knuckles P, Haussler U, Fabel K, Götz M *et al.* Quiescent and active hippocampal neural stem cells with distinct morphologies respond selectively to physiological and pathological stimuli and aging. *Cell Stem Cell* 2010; **6**: 445–456.
17. Gao Z, Ure K, Ding P, Nashaat M, Yuan L, Ma J *et al.* The master negative regulator REST/NRSF controls adult neurogenesis by restraining the neurogenic program in quiescent stem cells. *J Neurosci* 2011; **31**: 9772–9786.
18. Chakkalakal JV, Jones KM, Basson MA, Brack AS. The aged niche disrupts muscle stem cell quiescence. *Nature* 2012; **490**: 355–360.
19. Ruckh JM, Zhao JW, Shadrach JL, van Wijngaarden P, Rao TN, Wagers AJ *et al.* Rejuvenation of regeneration in the aging central nervous system. *Cell Stem Cell* 2012; **10**: 96–103.
20. Molofsky AV, Slutsky SG, Joseph NM, He S, Pardal R, Krishnamurthy J *et al.* Increasing p16 expression decreases forebrain progenitors and neurogenesis during ageing. *Nature* 2006; **443**: 448–452.
21. Mizumatsu S, Monje ML, Morhardt DR, Rola R, Palmer TD, Fike JR. Extreme sensitivity of adult neurogenesis to low doses of X-irradiation. *Cancer Res* 2003; **63**: 4021–4027.
22. Allen DM, van Praag H, Ray J, Weaver Z, Winrow CJ, Carter TA *et al.* Ataxia telangiectasia mutated is essential during adult neurogenesis. *Genes Dev* 2001; **15**: 554–566.
23. Blanpain C, Mohrin M, Sotiropoulou PA, Passegué E. DNA-damage response in tissue-specific and cancer stem cells. *Cell Stem Cell* 2011; **8**: 16–29.
24. Navarra P, Preziosi P. Hydroxyurea: new insights on an old drug. *Crit Rev Oncol Hematol* 1999; **29**: 249–255.
25. Park JI, Jeong JS, Han JY, Kim DI, Gao YH, Park SC *et al.* Hydroxyurea induces a senescence-like change of K562 human erythroleukemia cell. *J Cancer Res Clin Oncol* 2000; **126**: 455–460.
26. Yeo EJ, Hwang YC, Kang CM, Kim IH, Kim DI, Parka JS *et al.* Senescence-like changes induced by hydroxyurea in human diploid fibroblasts. *Exp Gerontol* 2000; **35**: 553–571.
27. Kahlem P, Dörken B, Schmitt CA. Cellular senescence in cancer treatment: friend or foe? *J Clin Invest* 2004; **113**: 169–174.
28. Adams PD. Healing and hurting: molecular mechanisms, functions and pathologies of cellular senescence. *Mol Cell* 2009; **36**: 2–14.
29. Antequera D, Vargas T, Ugalde C, Spuch C, Molina JA, Ferrer I *et al.* Cytoplasmic gelsolin increases mitochondrial activity and reduces Abeta burden in a mouse model of Alzheimer's disease. *Neurobiol Dis* 2009; **36**: 42–50.
30. Hebert-Chatelain E, Jose C, Gutierrez Cortes N, Dupuy JW, Rocher C, Dachary-Prigent J *et al.* Preservation of NADH ubiquinone-oxidoreductase activity by Src kinase-mediated phosphorylation of NDUFB10. *Biochim Biophys Acta* 2012; **1817**: 718–725.
31. Balsa E, Marco R, Perales-Clemente E, Szklarczyk R, Calvo E, Landázuri MO *et al.* NDUFA4 is a subunit of complex IV of the mammalian electron transport chain. *Cell Metab* 2012; **16**: 378–386.
32. Schlehe JS, Journel MS, Taylor KP, Amodeo KD, LaVoie MJ. The mitochondrial disease associated protein Ndufaf2 is dispensable for Complex-1 assembly but critical for the regulation of oxidative stress. *Neurobiol Dis* 2013; **58**: 57–67.
33. Jonckheere AI, Renkema GH, Bras M, van den Heuvel LP, Hoischen A, Gilissen C *et al.* A complex V ATP5A1 defect causes fatal neonatal mitochondrial encephalopathy. *Brain* 2013; **136**: 1544–1554.
34. Ressler S, Bartkova J, Niederegger H, Bartek J, Scharffetter-Kochanek K, Jansen-Dürr P *et al.* p16 is a robust in vivo biomarker of cellular aging in human skin. *Aging Cell* 2006; **5**: 379–389.
35. Neumann CA, Krause DS, Carman CV, Das S, Dubey DP, Abraham JL *et al.* Essential role for the peroxiredoxin PRDX1 in erythrocyte antioxidant defence and tumour suppression. *Nature* 2003; **424**: 561–565.
36. Turner-Ivey B, Manevich Y, Schulte J, Kistner-Griffin E, Jezierska-Drutel A, Liu Y *et al.* Role for Prdx1 as a specific sensor in redox-regulated senescence in breast cancer. *Oncogene* 2013; **32**: 5302–5314.
37. Hou Y, Ouyang X, Wan RQ, Cheng H, Mattson MP, Cheng A *et al.* Mitochondrial superoxide production negatively regulates neural progenitor proliferation and cerebral cortical development. *Stem Cells* 2012; **30**: 2535–2547.
38. Velarde MC, Flynn JM, Day NU, Melov S, Campisi J. Mitochondrial oxidative stress caused by Sod2 deficiency promotes cellular senescence and aging phenotypes in the skin. *Aging* 2012; **4**: 3–12.
39. Koopman WJ, Nijtmans LG, Dieteren CE, Roestenberg P, Valsecchi F, Smeitink JA *et al.* Mammalian mitochondrial complex I: biogenesis, regulation, and reactive oxygen species generation. *Antioxid Redox Signal* 2010; **12**: 1431–1470.
40. Schlehe JS, Journel MS, Taylor KP, Amodeo KD, Lavoie MJ. The mitochondrial disease associated protein Ndufaf2 is dispensable for Complex-1 assembly but critical for the regulation of oxidative stress. *Neurobiol Dis* 2013; **58**: 57–67.
41. Wallace DC. A mitochondrial paradigm of metabolic and degenerative diseases, aging, and cancer: a dawn for evolutionary medicine. *Annu Rev Genet* 2005; **39**: 359–407.
42. Naka K, Muraguchi T, Hoshii T, Hirao A. Regulation of reactive oxygen species and genomic stability in hematopoietic stem cells. *Antioxid Redox Signal* 2008; **10**: 1883–1894.
43. Freund A, Patil CK, Campisi J. p38MAPK is a novel DNA damage response-independent regulator of the senescence-associated secretory phenotype. *EMBO J* 2011; **30**: 1536–1548.
44. Ito K, Hirao A, Arai F, Takubo K, Matsuoka S, Miyamoto K *et al.* Reactive oxygen species act through p38 MAPK to limit the lifespan of hematopoietic stem cells. *Nat Med* 2006; **12**: 446–451.
45. Balaban RS, Nemoto S, Finkel T. Mitochondria, oxidants, and aging. *Cell* 2005; **120**: 483–495.
46. Rossi DJ, Seita J, Czechowicz A, Bhattacharya D, Bryder D, Weissman IL. Hematopoietic stem cell quiescence attenuates DNA damage response and permits DNA damage accumulation during aging. *Cell Cycle* 2007; **6**: 2371–2376.
47. Dimri GP, Lee X, Basile G, Acosta M, Scott G, Roskelley C *et al.* A novel biomarker identifies senescent human cells in culture and in aging skin in vivo. *Proc Natl Acad Sci USA* 1995; **92**: 9363–9367.

Supplementary Information accompanies this paper on Cell Death and Disease website (http://www.nature.com/cddis)